Colorization of the Visible Human Images

Bo Meng, Jian Yang, Danni Ai, Tianyu Fu
Beijing Engineering Research Center of Mixed Reality and Advanced Display, School of Optics and Electronics, Beijing Institute of Technology, Beijing 100081, China.
e-mail: jyang@bit.edu.cn

Ge Wang
Biomedical Imaging Center
Department of Biomedical Engineering
Rensselaer Polytechnic Institute
Troy, NY 12180, USA
e-mail: wangg6@rpi.edu

***Abstract* — The visible human project has created an authoritive set of tomographic images of the human bodies and helped various medical applications. This paper reports a method to turn the grey-scale CT images of the visible human into dual-/multi-energy counterparts. An image dataset from dual-energy CT scanner was registered to the visible human CT images using a non-rigid registration method, and the water- and bone-basis maps were fused by the estimated deformation field onto the visible human CT images. Then, the monochromatic image dataset at any KeV can be obtained from the mixture of the two basis materials. Then, it becomes feasible to estimate the two basis materials from the visible human CT atlas, and synthesize a standard spectral visible human CT dataset.**

Keywords* — *Visible human project, non-rigid registration, spectral CT

I. INTRODUCTION

The visible human project is an attempt to create cross-sectional images of the human body for anatomical visualization [1]. A dataset for the male body was completed in November 1994. Then, a counterpart for the female body was done in November 1995. The cadavers were "cut" through the axial plane at 1 mm interval. Each of the resulting "slices" was photographed in both analog and digital formats. The data were supplemented by axial tomographic sections of the whole body obtained by computed tomography (CT) and magnetic resonance imaging (MRI).

A General Electric High-Speed Advantage CT scanner was used to collect transverse images every millimeter through the head and neck; every 3 mm in the thorax, abdomen, and pelvis; and every 5 mm in the lower extremities at a fixed voltage of 120 kV and fixed tube current of 170 mA. This conventional CT scanner uses energy-integrating detectors in which x-ray photons are measured in terms of the total energy.

The problem with conventional CT is that it cannot material decomposition into basis functions, particularly in the cases of small lesions or other features of low contrast. This problem can be addressed through the advancement of dual-energy/spectral imaging [2-5]. By acquiring images at two different energy levels, dual-/multi-energy CT can differentiate various elements in the body.

In dual-energy CT, a set of images is generated with two x-ray spectra for use in diagnosis, similar to conventional polychromatic CT images but with doubled data. These dual-energy images can be processed to synthesize virtual monochromatic images. This approach was described in the original work by Alvarez and Macovski [6, 7], which involves a base material decomposition in the projection domain and a linear combination of the density maps of the base materials in the image domain. Another method is to linearly mix low- and high-energy images after respective image reconstructions [8-10].

In this study, we propose a novel method that non-rigidly registers a dataset from a dual-energy CT scanner to the visible human Project images. The estimated deformation field was used to warp water- and bone-based maps to the visible human dataset. Then, the monochromatic image dataset on any keV level can be obtained. Our simulation study indicates that the proposed method has the potential to obtain the two base materials from the visible human dataset and set up a standard spectral visible human dataset for clinical research.

II. METHODS

A. Monochromatic Images Using the Image-based Method

In dual-energy CT imaging, the linear attenuation coefficients with low- and high- energy spectra after image reconstruction can be expressed as a linear combination of the effective mass attenuation coefficients of the two base materials:

$$\begin{cases} \mu^L = (\frac{\mu}{\rho})_W^L \rho_W + (\frac{\mu}{\rho})_B^L \rho_B \\ \mu^H = (\frac{\mu}{\rho})_W^H \rho_W + (\frac{\mu}{\rho})_B^H \rho_B \end{cases} \quad (1)$$

where "L" and "H" represent low and high-energy respectively, "W" and "B" denote the two base materials, namely, water and bone, and $(\frac{\mu}{\rho})_i^j, i = 1,2; j = L,H$ indicates the effective mass attenuation coefficient of the two base materials for low- and high-energy scans respectively.

The mass density of the two base materials is obtained by solving the above two linear equations:

DOI: 10.12059/Fully3D.2017-11-3203037

$$\begin{cases} \rho_W = \dfrac{\mu^L \cdot (\dfrac{\mu}{\rho})_B^H - \mu^H \cdot (\dfrac{\mu}{\rho})_B^L}{\mathrm{M}} \\ \rho_B = \dfrac{-\mu^L \cdot (\dfrac{\mu}{\rho})_W^H + \mu^H \cdot (\dfrac{\mu}{\rho})_W^L}{\mathrm{M}} \end{cases} \tag{2}$$

where $\mathrm{M} = (\frac{\mu}{\rho})_W^L \cdot (\frac{\mu}{\rho})_B^H - (\frac{\mu}{\rho})_W^H \cdot (\frac{\mu}{\rho})_B^L$.

Then, the monochromatic image at energy E is given by

$$\mu(E) = (\frac{\mu}{\rho})_W(E)\rho_W + (\frac{\mu}{\rho})_B(E)\rho_B \tag{3}$$

Therefore, we can calculate the attenuation coefficient at any energy level using Eq. (3).

B. Non-rigid Registration to the Visible Human Dataset

Image registration is an important task in medical imaging. In many clinical situations, several patient images are obtained to analyze the patient's condition. These images are acquired under different conditions or using complementary modalities. The combination of patient datasets, which can be mono- or multimodal, often yields additional clinical information that is not apparent in the separate images. Therefore, the spatial relation between the images needs to be determined. For this purpose, a spatial one-to-one mapping must be estimated between the two images.

In this study, non-rigid registration is conducted using the open-source software package Elastix [11, 12], including several optimization methods, multiresolution schemes, interpolators, transformation models, and cost functions. Elastix is a command line program, and the basic command to run a registration is as follows:

elaxtix –f fixedImage.ext –m movingImage.ext –out outputDirectory –p parameterFile.txt

where "fixedImage.ext" represents the dataset from the visible human Project, "movingImage.ext" represents the dataset from a patient, and the parameter file contains, in normal text, the types of registration performed (i.e., what metric and optimizer) and the parameters that define the registration (Table I).

Table I. Non-rigid registration parameters.

Registration method	Multi-Resolution Registration
Interpolator	BSpline Interpolator
Resample Interpolator	Final BSpline Interpolator
Optimizer	Adaptive Stochastic Gradient Descent
Transform	BSpline Transform
Metric	Advanced Mattes Mutual Information

C. Spectralization of the Visible Human Dataset

To obtain a density map of two base materials for the Visible Human dataset, we applied the deformation field estimated in non-rigid registration to the water- and bone-based maps of the patient dataset. Then, we generated images at various energy levels for the Visible Human dataset.

III. Simulation Results

Two CT datasets were used to evaluate the proposed technique. The patient was scanned by a dual-energy CT scanner. The other dataset is the visible man CT dataset from the visible human project.

CT slices from the patient dataset in Fig. 1 were defined on a 512 × 512 grid, acquired at the tube potential of 50 and 100 kV respectively. We have:

$$\begin{cases} \mu^{50kV} = (\dfrac{\mu}{\rho})_W^{50kV}\rho_W + (\dfrac{\mu}{\rho})_B^{50kV}\rho_B \\ \mu^{100kV} = (\dfrac{\mu}{\rho})_W^{100kV}\rho_W + (\dfrac{\mu}{\rho})_B^{100kV}\rho_B \end{cases} \tag{4}$$

where μ^{50kV} and μ^{100kV} are the attenuation coefficients at 50kV and 100kV respectively, as shown in Fig.1.

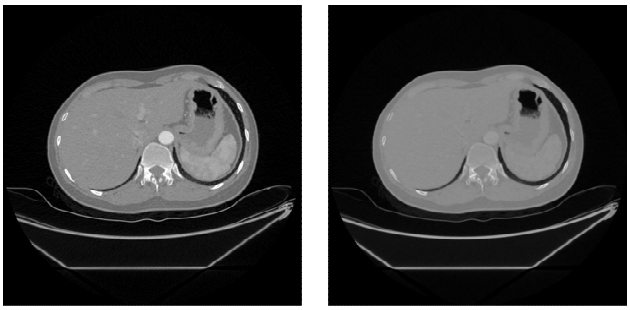

(a) (b)

Figure 1. Reconstructed images at low- and high-energy spectra respectively. (a) A reconstructed image at 50kV, displayed in [0,2000]HU; and (b) the reconstructed image at 100kV, displayed in [0,2000]HU.

Clearly,

$$\begin{cases} \rho_W = \dfrac{\mu^{50kV} \cdot (\dfrac{\mu}{\rho})_B^{100kV} - \mu^{100kV} \cdot (\dfrac{\mu}{\rho})_B^{50kV}}{\mathrm{M}} \\ \rho_B = \dfrac{-\mu^{50kV} \cdot (\dfrac{\mu}{\rho})_W^{100kV} + \mu^{100kV} \cdot (\dfrac{\mu}{\rho})_W^{50kV}}{\mathrm{M}} \end{cases} \tag{5}$$

where $\mathrm{M} = (\frac{\mu}{\rho})_W^{50kV} \cdot (\frac{\mu}{\rho})_B^{100kV} - (\frac{\mu}{\rho})_W^{100kV} \cdot (\frac{\mu}{\rho})_B^{50kV}$.

With Eq. (5), we can calculate the density map of two basis materials: water and bone, as shown in Fig. 2. The monochromatic image at 40keV, 60keV, 70keV and 80keV can

be easily calculated by inserting the density maps of two basis materials into Eq. (3), as shown in Fig. 3.

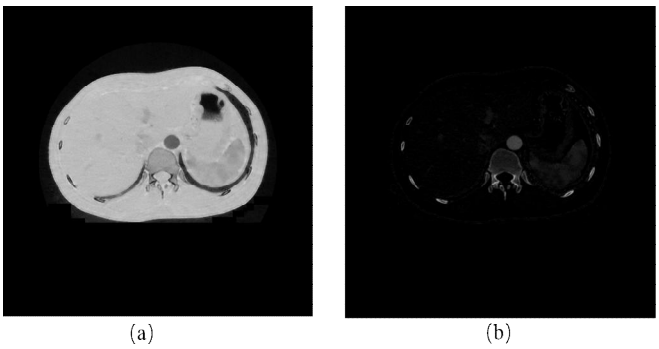

Figure 2. Destiny maps of the two basis materials. (a) The destiny map of water, displayed in [0,1.5]; and (b) the destiny map of bone displayed in [0,1.5].

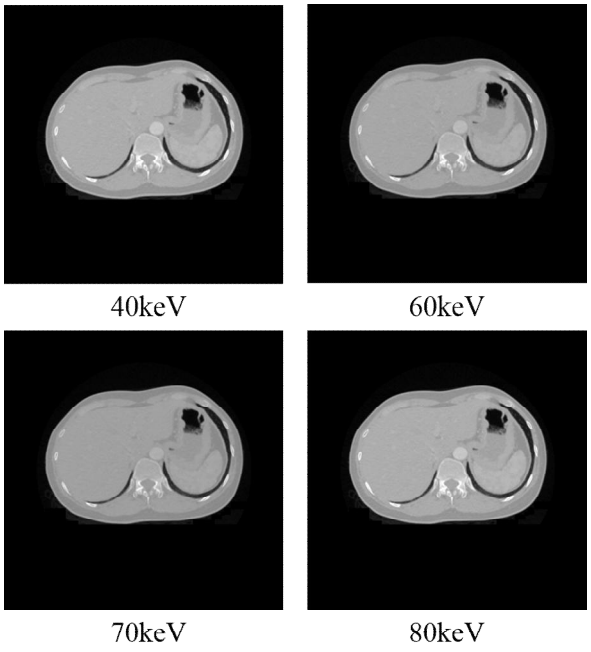

Figure 3. Monochromatic CT images synthesized at different keV settings.

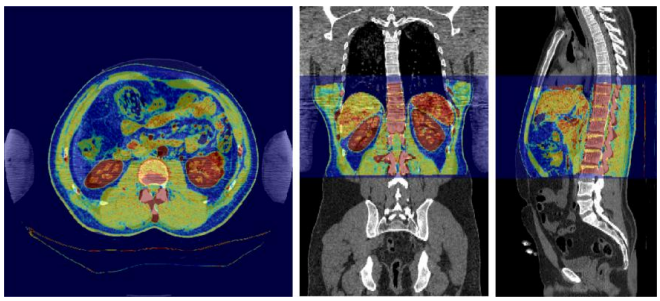

Figure 4. Non-rigid registration of a patient dataset into the visible human dataset. The colorized image is the warped patient dataset, while the grey image is the visible human dataset.

The registration results are visually and quantitatively satisfactory, as shown in Fig. 4. The deformation field estimated by non-rigid registration was then applied to warp the two base materials of the patient dataset to estimate the two base materials for the visible man dataset, as illustrated in Fig. 5.

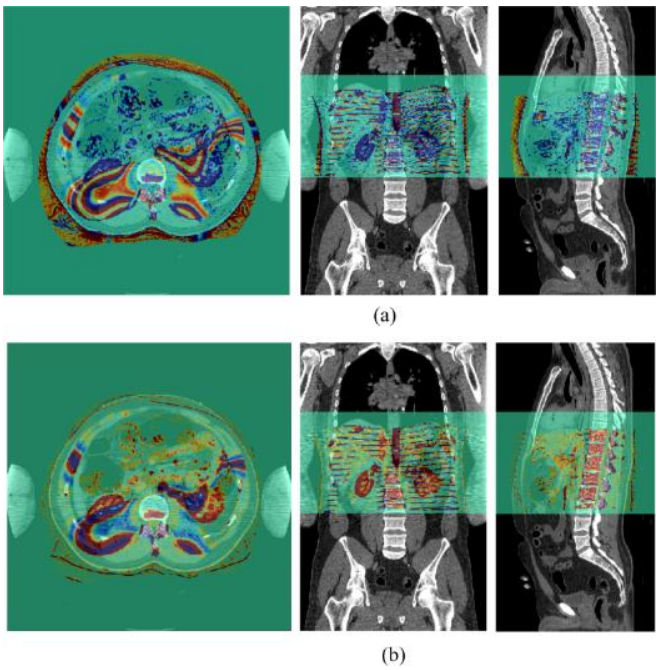

Figure 5. Warped water and bone maps on the visible human dataset. (a) The colorized image is the warped water map, while the grey image is the visible man dataset; and (b) the colorized image is the warped bone map, while the grey image is again the visible man dataset.

IV. DISCUSSIONS AND FUTURE WORK

Extensive previous studies were well documented based on the datasets from the visible human Project. For example, the VH Dissector from Touch of Life Technologies and Voxel-Man 3D Navigator from the University of Hamburg. However, the visible human dataset was acquired using a conventional CT scanner without spectral information, thereby limiting the utilities of the datasets.

In this study, we have proposed a novel method to spectralize the visible human dataset. A transformation matrix generated by a non-rigid registration operation was used to transfer the water- and bone-based maps from a patient to the visible human CT images. The preliminary results indicate the feasibility of the proposed spectralization method. A future research topic is to evaluate how such a colorization of the visible human images would depend on the choice of the patient dataset. Also, we can expand this method to spectralize any dataset scanned by a conventional CT.

It has been found that the non-rigid registration of a patient CT dataset to the visible human dataset is promising. The simulation results show that the roadmap to spectralize the visible human dataset is clear, and can be further refined. Our proposed method offers an innovative solution for the spectralization of the visible human dataset. With our colorized results as the initial guess, dual-energy CT images could be better reconstructed (see the paper by Cong WX et al, and the paper by Wang YM et al. in this proceedings).

ACKNOWLEDGEMENT

This work was partially supported by the National Hi-Tech Research and Development Program (2015AA043203), and the National Science Foundation Program of China (61672099, 81430039, 61527827, 61501030, 61572076, U153310181), and the NIH/NIBIB (U01 EB017140).

REFERENCES

[1] V. Spitzer, M. J. Ackerman, A. L. Scherzinger, and D. Whitlock, "The visible human male: a technical report," Journal of the American Medical Informatics Association, vol. 3, no. 2, pp. 118-130, 1996.

[2] C. A. Coursey et al., "Dual-Energy Multidetector CT: How Does It Work, What Can It Tell Us, and When Can We Use It in Abdominopelvic Imaging?," Radiographics, vol. 30, no. 4, pp. 1037-1055, Jul-Aug 2010.

[3] F. Dilmanian et al., "Single-and dual-energy CT with monochromatic synchrotron x-rays," Physics in medicine and biology, vol. 42, no. 2, p. 371, 1997.

[4] T. R. Johnson et al., "Material differentiation by dual energy CT: initial experience," European radiology, vol. 17, no. 6, pp. 1510-1517, 2007.

[5] B. M. Yeh, J. A. Shepherd, Z. J. Wang, H. S. Teh, R. P. Hartman, and S. Prevrhal, "Dual-energy and low-kVp CT in the abdomen," American Journal of Roentgenology, vol. 193, no. 1, pp. 47-54, 2009.

[6] R. E. Alvarez and A. Macovski, "Energy-Selective Reconstructions in X-Ray Computerized Tomography," Physics in Medicine and Biology, vol. 21, no. 5, pp. 733-744, 1976.

[7] L. A. Lehmann et al., "Generalized Image Combinations in Dual Kvp Digital Radiography," Medical Physics, vol. 8, no. 5, pp. 659-667, 1981.

[8] L. Yu, J. A. Christner, S. Leng, J. Wang, J. G. Fletcher, and C. H. McCollough, "Virtual monochromatic imaging in dual-source dual-energy CT: radiation dose and image quality," Med Phys, vol. 38, no. 12, pp. 6371-9, Dec 2011.

[9] L. Yu, S. Leng, and C. H. Mccollough, "Dual-energy CT-based monochromatic imaging," Ajr American Journal of Roentgenology, vol. 199, no. 5 Suppl, p. S9, 2012.

[10] K. Tokumori et al., "Monochromatic X-Ray Ct Using Fluorescent X-Rays Excited By Synchrotron Radiation," Engineering in Medicine & Biology Society Proceedings of Annual International Conf, vol. 4, no. 4, pp. 2987 - 2989, 2000.

[11] S. Klein, M. Staring, K. Murphy, M. A. Viergever, and J. P. Pluim, "Elastix: a toolbox for intensity-based medical image registration," IEEE transactions on medical imaging, vol. 29, no. 1, pp. 196-205, 2010.

[12] M. Staring, S. Klein, J. H. Reiber, W. J. Niessen, and B. C. Stoel, "Pulmonary image registration with elastix using a standard intensity-based algorithm," Medical Image Analysis for the Clinic: A Grand Challenge, pp. 73-79, 2010.